

Article

Electrochemical Sensor for Cu(II) Based on Carbon Nanotubes Functionalized with a Rationally Designed Schiff Base

Alejandro Tamborelli ^{1,2,†}, Michael López Mujica ^{2,†}, Gustavo Servetti ¹, Diego Venegas-Yazigi ^{3,4} ,
Patricio Hermosilla-Ibáñez ^{3,4,*} , Pablo Dalmasso ^{1,*}  and Gustavo Rivas ^{2,*}

¹ CIQA, CONICET, Departamento de Ingeniería Química, Facultad Regional Córdoba, Universidad Tecnológica Nacional, Maestro López esq. Cruz Roja Argentina, 5016 Córdoba, Argentina; alejandrotamborelli@gmail.com (A.T.); gservetti@frc.utn.edu.ar (G.S.)

² INFIQC, CONICET-UNC, Departamento de Físicoquímica, Facultad de Ciencias Químicas, Universidad Nacional de Córdoba, Ciudad Universitaria, 5000 Córdoba, Argentina; mlopezmujica@unc.edu.ar

³ Departamento de Química de los Materiales, Facultad de Química y Biología, Universidad de Santiago de Chile, Santiago 9170022, Chile; diego.venegas@usach.cl

⁴ Centro para el Desarrollo de la Nanociencia y la Nanotecnología (CEDENNA), Universidad de Santiago de Chile, Santiago 9170022, Chile

* Correspondence: patricio.hermosilla@usach.cl (P.H.-I.); pdalmasso@frc.utn.edu.ar or p-dalmasso@hotmail.com (P.D.); gustavo.rivas@unc.edu.ar (G.R.)

† These authors contributed equally to this work.

Abstract: This work proposes a new strategy for the electrochemical quantification of Cu(II) using glassy carbon electrodes (GCEs) modified with a nanohybrid of multiwall carbon nanotubes (MWCNTs) non-covalently functionalized with a rationally designed Schiff base containing different groups (SB-dBA). The principle of sensing was the complexation of Cu(II) by the Schiff base that supports the MWCNTs at the open-circuit potential, followed by a reduction step at -0.600 V and further linear sweep anodic stripping voltammetry (LSASV) in a 0.200 M acetate buffer solution of pH 5.00. The linear range goes from 10 to 200 $\mu\text{g L}^{-1}$, with a sensitivity of (0.79 ± 0.07) $\mu\text{A L } \mu\text{g}^{-1}$ ($R^2 = 0.991$), a detection limit of 3.3 $\mu\text{g L}^{-1}$, and a reproducibility of 8.0% for the same nanohybrid (nine electrodes) and 9.0% for four different nanohybrids. The proposed sensor was very selective for Cu(II) even in the presence of Pb(II), Fe(II), As(III), Cr(III), Cd(II), and Hg(II), and it was successfully used for the quantification of Cu(II) in different water samples (tap, groundwater, and river) without any pretreatment.

Keywords: copper; electrochemical sensor; multiwall carbon nanotubes; Schiff base; carbon nanotube dispersion; non-covalent functionalization; complexation



Received: 29 November 2024

Revised: 4 January 2025

Accepted: 12 January 2025

Published: 25 January 2025

Citation: Tamborelli, A.; López Mujica, M.; Servetti, G.; Venegas-Yazigi, D.; Hermosilla-Ibáñez, P.; Dalmasso, P.; Rivas, G.

Electrochemical Sensor for Cu(II) Based on Carbon Nanotubes Functionalized with a Rationally Designed Schiff Base. *Chemosensors* **2025**, *13*, 35. <https://doi.org/10.3390/chemosensors13020035>

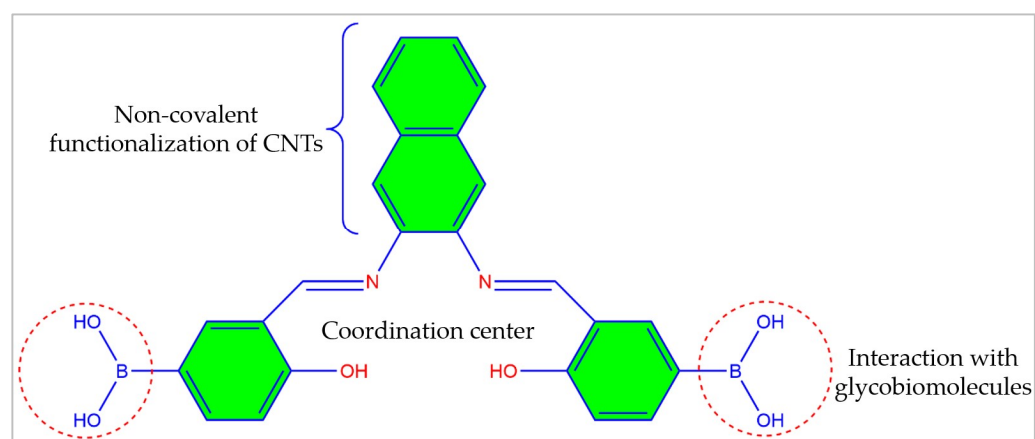
Copyright: © 2025 by the authors. Licensee MDPI, Basel, Switzerland. This article is an open access article distributed under the terms and conditions of the Creative Commons Attribution (CC BY) license (<https://creativecommons.org/licenses/by/4.0/>).

1. Introduction

The incorporation of carbon nanotubes (CNTs) to different electrodes has been demonstrated to be highly successful not only in improving the sensing performance but also in facilitating the assembly of different (bio)sensor constituents [1–3]. The surface functionalization of CNTs is a crucial aspect to ensure an efficient response of the resulting sensors [4,5]. In this regard, the rational selection of the compound used to non-covalently functionalize CNTs makes possible the successful disaggregation of the nanostructures and confers them particular properties depending on the nature of the compound used as the functionalizing agent [6–10].

Organic molecules of the Schiff base (SB) type have been widely used as ligands in coordination chemistry. They are classified according to the number and type of donor

atoms present in the chemical structure, the most common being nitrogen and oxygen, and just in a few cases, phosphorus and sulfur. The design and synthesis of new chelating platforms based on SBs allow the development of diverse multifunctional systems, which, according to the nature of the ligands, have been used in different fields like sensors, catalysis, energy, and medicine [11–14], among others. Recently, we have synthesized a new SB, (((1E,1'E)-(naphthalene-2,3-diylbis(azaneylylidene))bis(methaneylylidenedene))bis(4-hydroxy-3,1-phenylene))diboronic acid called SB-dBA [15], which presents various functional groups in its chemical structure (Scheme 1): (i) a coordination center for metallic ions of type N_2O_2 , (ii) boronic acid groups available for the interaction with glyco-biomolecules, and (iii) an aromatic organic skeleton to allow the non-covalent functionalization of CNTs via π - π stacking interaction. In this sense, we have recently reported the non-covalent functionalization of multiwall carbon nanotubes (MWCNTs) with this rationally designed SB-dBA to obtain a MWCNT-SB-dBA nanohybrid with properties mimicking the specific interaction of lectines with glyco-compounds. The nanohybrid was used in two directions, for the development of a hydrogen peroxide biosensor through the immobilization of horseradish peroxidase (HRP) at glassy carbon electrodes (GCEs) modified with MWCNT-SB-dBA [15], and for the preparation of a glucose biosensor after anchoring a mixture of HRP and glucose oxidase (GOx) on nanohybrid-modified GCEs [16].



Scheme 1. Functional groups in the chemical structure of SB-dBA ligand. Inside the circles are the boronic substituents and, in green color, the aromatic rings of the ligand.

A recent search in the CCDC crystallographic database (ConQuest version 2024.1.0) [17] based on the $Cu-N_2O_2$ -type fragment formed by aromatic rings and copper showed interesting results. Among the 133 reported crystalline structures, 115 display a coordination sphere around the $Cu(II)$ ion as square planar, and only in a few cases, $Cu(II)$ is penta- or hexa-coordinated since the metallic center completes its first coordination sphere with solvent molecules or with the counter-ion of the metallic salts (Scheme 1). Based on this information, we took advantage of the coordination ability of the N_2O_2 center to design a new strategy for the preparation of an electrochemical $Cu(II)$ sensor. The novelty of the work proposed here is the use of the nanohybrid resulting from the non-covalent functionalization of MWCNTs with the rationally designed SB-dBA deposited at GCEs as a platform to selectively preconcentrate $Cu(II)$ by complex formation at the open-circuit potential, in order to improve in an easy way the sensitivity of $Cu(II)$ quantification. $Cu(II)$ is an essential heavy metal present in numerous and important enzymes that play a key role in life [18] but, at the same time, it is a prevalent pollutant in the environment that at high concentrations can cause hazardous effects on plants, animals, and humans, and affect drinking water standards (World Health Organization WHO guideline = 2.0 mg L^{-1}) [19,20]. The excessive intake of $Cu(II)$ can be responsible for several health problems such as cirrhosis,

kidney failure, and Alzheimer's disease, among others [21]. Therefore, it is highly necessary to develop new, simple, sensitive, selective, and user-friendly sensing methodologies for Cu(II), capable of being used even in underdeveloped countries where it is difficult to obtain very sophisticated equipment.

The preconcentration of Cu(II) on electrode surfaces has been demonstrated to be a very important analytical tool to enhance the performance of the resulting sensors. In this sense, diverse strategies have been proposed like the use of chelating agents, metal–organic frameworks (MOF), ion-imprinted polymers, and compounds that facilitate electrostatic interaction, among others. Different chelating agents immobilized on electrode surfaces have been successfully used to improve Cu(II) quantification, such as dopamine (DA) adsorbed on a carbon ceramic electrode (CCE) [22], 2-mercaptobenzothiazole (MBT) incorporated within a carbon paste electrode (CPE) [23], dimercaptosuccinic acid (DMSA) immobilized on magnetic polydopamine ($\text{Fe}_3\text{O}_4\text{@PDA}$) [24], bathocuproinedisulfonic acid (BCS) used as an exfoliating agent of MWCNTs [25], bis(3-((5-mercapto-1,3,4-thiadiazol-2-yl)carbamoyl)phenyl)terephthalate (BMTCPT) as a chelating dithiol self-assembled on a gold electrode (AuE) or incorporated within CPE previous immobilization on gold nanoparticles (AuNPs) [26], and aluminon (aurintricarboxylic acid ammonium salt, ATA) as a chelating ionophore electrodeposited on a magnetic bead (MB)-modified GCE [27].

Regarding the use of MOFs, suspensions of Bi-MOF [28], UiO-66- NH_2 -ZnO nanocomposite [29], and Zn/Ni-ZIF-8-XC72-Nafion hybrid [30] have also been reported for the successful electrochemical determination of Cu(II). The application of ion-imprinted polymers obtained from the electropolymerization of p-phenylenediamine (PPD) as a template [31], the precipitation polymerization of methacrylamido-L-histidine (MAH) as a functional monomer using ethylene glycol dimethacrylate (EGDMA) as crosslinker [32], or the use of a L-cysteine-grafted chitosan (Cys-CTS) dropped on nitrogen-doped reduced graphene oxide (N-rGO) as the functional monomer [33] have also been reported for the preconcentration and effective quantification of Cu(II). A composite of sodium carboxymethyl cellulose (CMC) and Nafion [34] and activated biochar (aBC) prepared from sugarcane bagasse [35] were reported as other alternatives for Cu(II) accumulation via electrostatic interaction.

Bakhsh et al. [36] reported an amperometric sensor based on a core–shell nanomaterial of ZnSe-CdSe nanoparticles coated with SiO_2 . Noroozi et al. [37] proposed a CPE-MWCNT modified with amine-functionalized mesoporous Fe_3O_4 nanoparticles (NH_2 -meso- Fe_3O_4) using indigo carmine (IC) as an electrochemical mediator. Moreover, an ion-selective electrode for Cu(II) detection was proposed by Gupta et al. using CuS particles trapped in a polyvinyl chloride (PVC) matrix [38].

In the following sections, we discuss the optimization of the experimental conditions to prepare the voltammetric Cu(II) sensor as well as the analytical performance and the practical applications of the resulting sensor.

2. Materials and Methods

2.1. Reagents

Multiwall carbon nanotubes (MWCNTs, diameter (30 ± 15) nm, length 1–5 μm) were obtained from Sigma-Aldrich (St. Louis, MO, USA). Acetic acid and sodium acetate were purchased from J.T.Baker (Center Valley, PA, USA). Copper(II) sulfate pentahydrate, arsenic(III) oxide, and mercury(II) nitrate monohydrate were acquired from Biopack (Zárate, Buenos Aires, Argentina). Lead(II) nitrate, iron(II) sulfate heptahydrate, and cadmium sulfate octahydrate were purchased from Anhedra (Troncos del Talar, Buenos Aires, Argentina). Chromium(III) nitrate nonahydrate was provided by Merck KGaA (Darmstadt, Germany). Other chemicals were reagent-grade and used without further purification.

Ultrapure water (resistivity = 18.2 M Ω ·cm) from a Millipore-MilliQ system (Molsheim, France) was used to prepare all aqueous solutions.

2.2. Apparatus

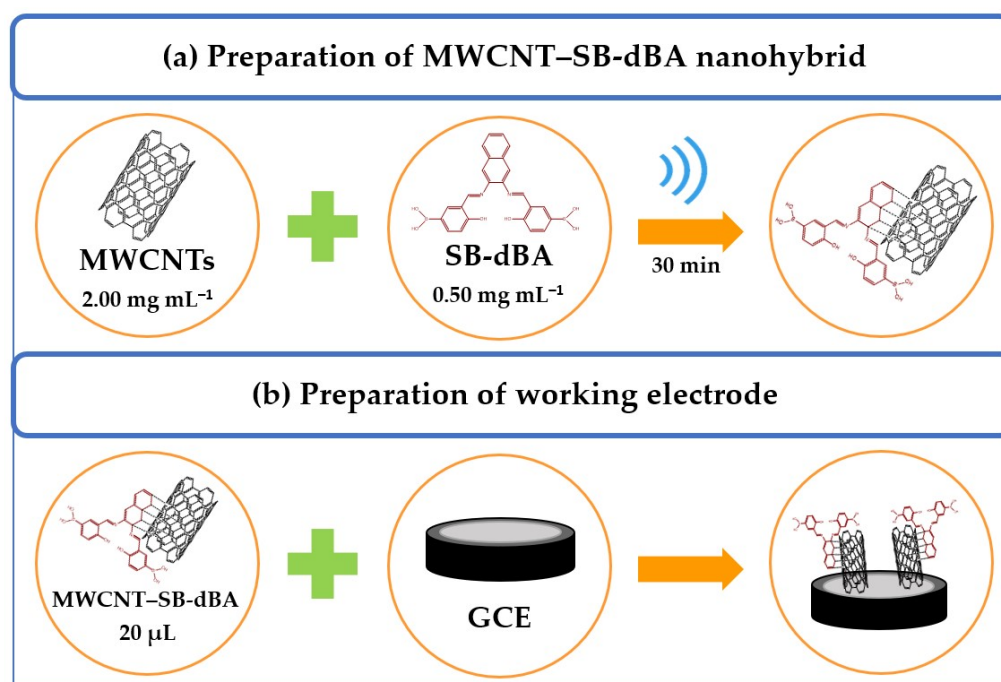
Electrochemical experiments were carried out with a TEQ_4 potentiostat (nanoTeq, Buenos Aires, Argentina) using the typical three-electrode system. A platinum wire was used as the auxiliary electrode, while a Ag/AgCl (3 M NaCl) (BASi, West Lafayette, IN, USA) was the reference electrode, and a glassy carbon electrode (GCE) modified with the MWCNT-SB-dBA nanohybrid was the working electrode (electroactive area of 73 mm²). The potentials are referenced to Ag/AgCl (3 M NaCl). Linear sweep voltammetry (LSV) experiments were carried out in a 0.200 M acetate buffer solution of pH 5.00 at 0.100 V s⁻¹. All measurements were performed at room temperature. The convective transport during the complexation step was provided by a magnetic stirrer (C-3 Cell Stand, BASi, West Lafayette, IN, USA) at 800 rpm.

An ultrasonic cleaner (TB04TA, Testlab, Bernal, Argentina) of 40 kHz frequency and 160 W of ultrasonic power was used for performing the sonication treatments.

Scanning Electron Microscopy (SEM) images were obtained using a FE-SE Sigma-ZEISS microscope (Cambridge, UK) with secondary and back-scattered electron detectors and equipped with an energy dispersive X-ray spectroscopy (EDX) analysis system. The samples were prepared by reduction of previously accumulated Cu(II) at glassy carbon disks (GCDs) modified with MWCNT-SB-dBA.

2.3. Preparation of GCE Modified with MWCNT-SB-dBA Nanohybrid

MWCNT-SB-dBA nanohybrid was prepared according to Tamborelli et al. [15]. Briefly, 2.00 mg of MWCNTs were first mixed with 0.50 mg SB-dBA ligand (dissolved in 1.00 mL of N,N-dimethylformamide (DMF)), and the resulting mixture was sonicated with an ultrasonic bath for 30 min (Scheme 2a).

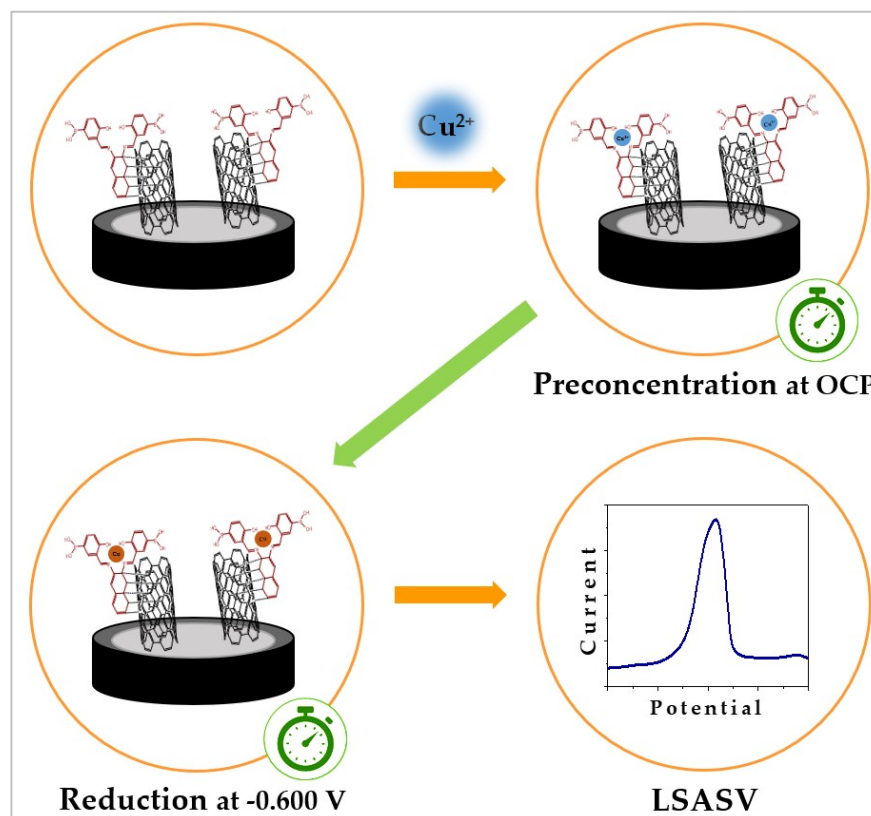


Scheme 2. Representation of the construction of the electrochemical sensor for Cu(II) based on the use of the MWCNT-SB-dBA nanohybrid immobilized at GCE.

The GCEs modified with the nanohybrid (GCE/MWCNT-SB-dBA) were prepared by deposition of 20 μL of the nanohybrid at the GCE surface, which was previously polished (with alumina slurries of 1.0, 0.3, and 0.05 μm) and water-sonicated. Once the solvent (DMF) was evaporated at room temperature, the electrode was ready to use (Scheme 2b).

2.4. Procedure

The Cu(II) quantification consisted of the following steps (Scheme 3):



Scheme 3. Representation of the different steps for the electrochemical sensing of Cu(II). The first step (orange arrow) is the coordination of Cu(II), the second step (green arrow) is the reduction of the accumulated Cu(II), and the third step is the reoxidation of copper.

- (i) Preconcentration of Cu(II): accomplished by dipping GCE/MWCNT-SB-dBA in a stirred Cu(II) solution (prepared in a 0.200 M acetate buffer solution of pH 5.00) for a given time at open-circuit potential (ocp) to preconcentrate it by complex formation. Once the Cu(II) was complexed at the electrode surface, it was washed with the acetate buffer solution.
- (ii) Reduction of the complexed Cu(II): after preconcentrating the Cu(II) by complex formation, the electrode was transferred to a fresh acetate buffer solution, and the complexed Cu(II) was reduced by applying -0.600 V for 5 min.
- (iii) Electrochemical analysis: carried out in acetate buffer solution by linear sweep anodic stripping voltammetry (LSASV) between -0.300 V and 0.300 V at 0.100 V s⁻¹.

Tap water samples were obtained from the laboratory, groundwater samples were extracted using a windmill, and river water samples were collected from the Suquía river (Córdoba city, Argentina). The samples were used without pretreatment and enriched with different volumes of the Cu(II) stock solution.

3. Results and Discussion

3.1. Electrochemical Behavior of Cu(II) Accumulated at Different Electrodes

Figure 1 shows linear sweep voltammograms obtained at GCE/MWCNT–SB–dBA (a), GCE/MWCNTs (b) and bare GCE (c) in a 0.200 M acetate buffer solution of pH 5.00 after 20 min interaction with $50 \mu\text{g L}^{-1}$ Cu(II) at ocp followed by 5 min of reduction at -0.600 V in a fresh acetate buffer solution. A clearly defined oxidation peak is obtained at GCE/MWCNT–SB–dBA due to the complexation of Cu(II) with the SB–dBA that supports the MWCNTs (peak potential (E_p) = -0.107 V, peak current (i_p) = $47 \mu\text{A}$). A considerably smaller response was obtained at the GCE/MWCNTs (E_p = -0.105 V, i_p = $6 \mu\text{A}$), demonstrating the key role of the ligand to preconcentrate Cu(II). A negligible response at more elevated potentials (E_p = 0.041 V; i_p = $0.7 \mu\text{A}$) is obtained at bare GCE due to the poor accumulation of Cu(II).

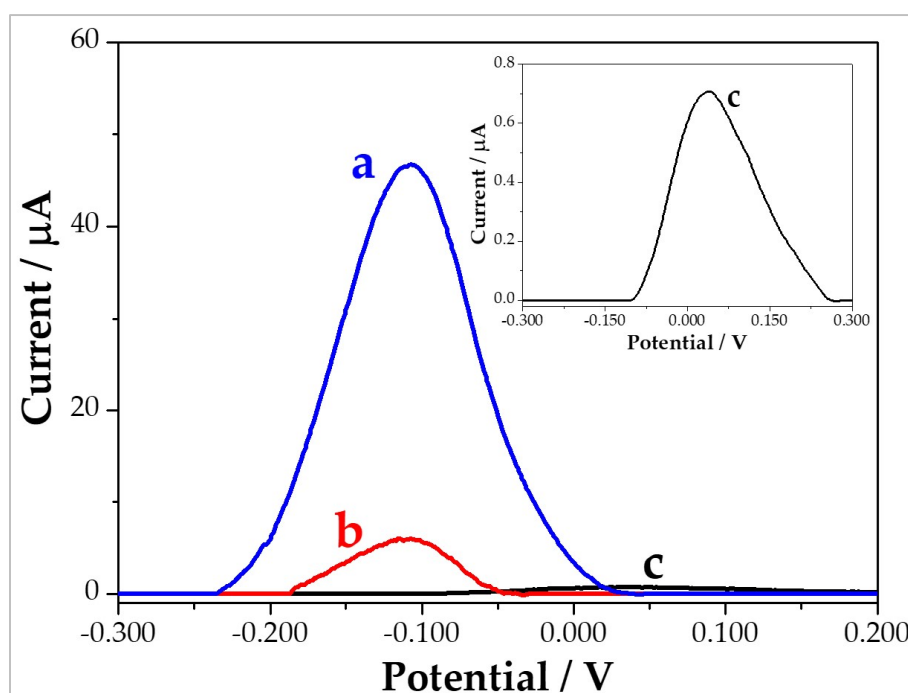


Figure 1. Linear sweep anodic stripping voltammograms for $50 \mu\text{g L}^{-1}$ Cu(II) obtained at GCE/MWCNT–SB–dBA (a, blue line), GCE/MWCNTs (b, red line), and GCE (c, black line). The inset shows a zoom of the LSASV at bare GCE. Accumulation time: 20 min. Reduction potential: -0.600 V. Reduction time: 5 min. Scan rate: 0.100 V s^{-1} . Supporting electrolyte: 0.200 M acetate buffer solution, pH 5.00.

3.2. Optimization of Cu(II) Preconcentration and Reduction at GCE/MWCNT–SB–dBA

The interaction time of Cu(II) with GCE/MWCNT–SB–dBA is a critical parameter for the preconcentration of the cation. Figure 2A displays the effect of the interaction time of $50 \mu\text{g L}^{-1}$ Cu(II) on the oxidation peak current of the preconcentrated and reduced copper. As the interaction time increases from 5 to 20 min, the oxidation peak currents show an important increment. For longer times, this increment is lower due to the saturation of the available N_2O_2 -type centers for complexation. Therefore, the selected time was 20 min.

The conditions for the reduction of the preconcentrated Cu(II) are also important to ensure a sensitive response. Different potentials were applied to reduce the complexed Cu(II) at MWCNT–SB–dBA between -0.400 V and -0.900 V. High negative potentials generate bubbles due to the hydrogen evolution producing non-reproducible analytical signals. A potential of -0.600 V was selected as the optimum since it allowed both the complete reduction of the accumulated copper and a reproducible and sensitive analytical signal. Figure 2B depicts the effect of the time for the reduction of the complexed Cu(II) at

−0.600 V on the analytical performance of the sensor. As this reduction time increases, the oxidation peak current also increases due to the efficient reduction of complexed Cu(II), with 5 min providing the best compromise between sensitivity and reproducibility.

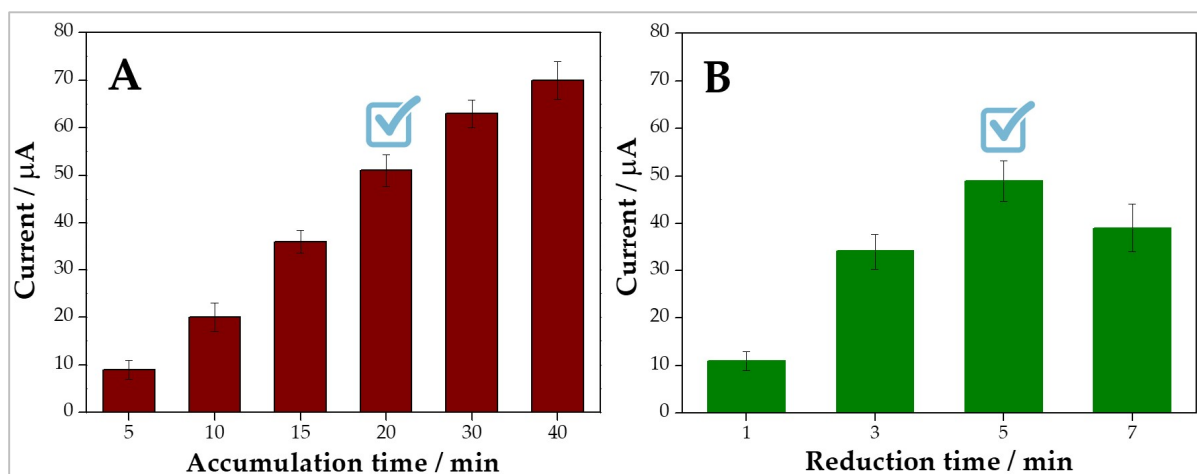


Figure 2. Influence of the accumulation time (A) and the reduction time (B) on the LSASV response of $50 \mu\text{g L}^{-1}$ Cu(II) at GCE/MWCNT-SB-dBA. Other experimental conditions as in Figure 1.

3.3. SEM-EDX Characterization of Cu(II) Complexed and Reduced at GCE/MWCNT-SB-dBA

Figure 3A displays a representative SEM image of glassy carbon disks (GCDs) modified with MWCNT-SB-dBA after reduction for 5 min at −0.600 V of Cu(II) complexed/accumulated for 20 min at ocp from a $250 \mu\text{g L}^{-1}$ Cu(II) solution prepared in acetate buffer solution. Based on this image, the distribution of the exfoliated MWCNTs follows the typical pattern of glassy carbon surfaces modified with nanohybrids obtained by the non-covalent functionalization of MWCNTs, covering the whole surface and showing areas with a higher density of carbon nanostructures.

In order to confirm the presence of copper, EDX measurements were performed, with the results displayed in Figure 3B,C. The EDX map for Cu shows a clear distribution of this element on the entire surface of GCD/MWCNT-SB-dBA (Figure 3B), in agreement with the EDX spectrum where a Cu peak (K line) appears at 8.05 KeV (Figure 3C), clearly demonstrating the presence of Cu after complexation with the SB-dBA ligand that supports the CNTs and its reduction on the GCD surface.

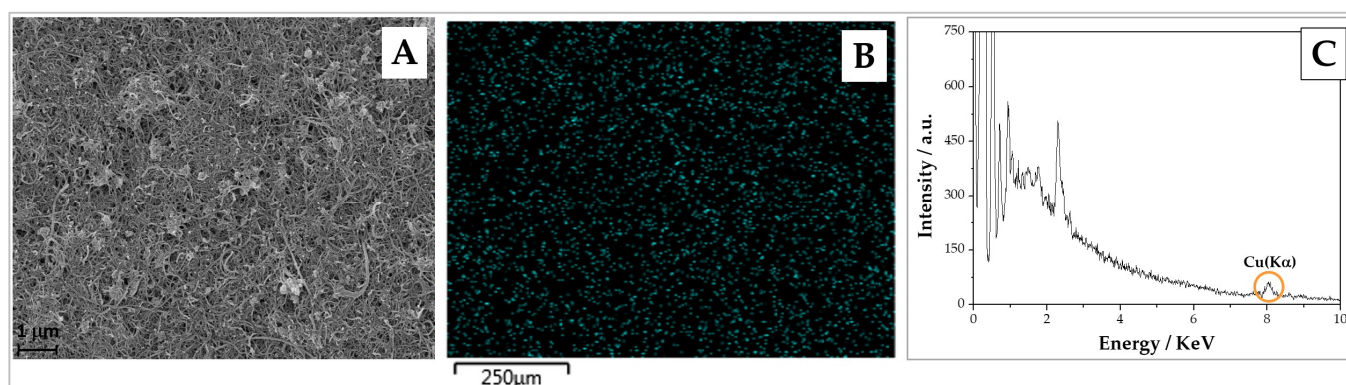


Figure 3. (A) SEM image of a glassy carbon disk (GCD) modified with MWCNT-SB-dBA after the reduction of previously accumulated Cu(II) from a $250 \mu\text{g L}^{-1}$ Cu(II) solution in 0.200 M acetate buffer solution, pH 5.00 (accumulation time: 20 min; accumulation potential: ocp; reduction time: 5 min; reduction potential: −0.600 V). (B) EDX map for Cu after Cu(II) reduction on GCD/MWCNT-SB-dBA. (C) EDX spectrum showing the presence of Cu (K line) at 8.05 KeV on GCD/MWCNT-SB-dBA.

3.4. Analytical Application of GCE/MWCNT-SB-dBA for Cu(II) Sensing

Figure 4 displays the LSASV response for different concentrations of Cu(II) between 10 and 250 $\mu\text{g L}^{-1}$, with well-defined signals for all the Cu(II) concentrations evaluated. The inset depicts the corresponding calibration plot, which shows a linear dependence between the oxidation peak current at around -0.100 V and Cu(II) concentration between 10 and 200 $\mu\text{g L}^{-1}$, with a sensitivity of $(0.79 \pm 0.07)\ \mu\text{A L}\ \mu\text{g}^{-1}$ ($R^2 = 0.991$), a reproducibility of 8.0% for the same nanohybrid (nine electrodes), and 9.0% for four different nanohybrids. The detection limit was of 3.3 $\mu\text{g L}^{-1}$ (taken as $3.3 \times \sigma/S$, where σ is the standard deviation of the blank signal and S , the sensitivity) and the quantification limit was 10 $\mu\text{g L}^{-1}$ (taken as $10 \times \sigma/S$). It is important to mention that the maximum Cu(II) level allowed in drinking water by the WHO, which is 2.0 mg L^{-1} [19,20]), is considerably higher than the values detected with our GCE/MWCNT-SB-dBA sensor.

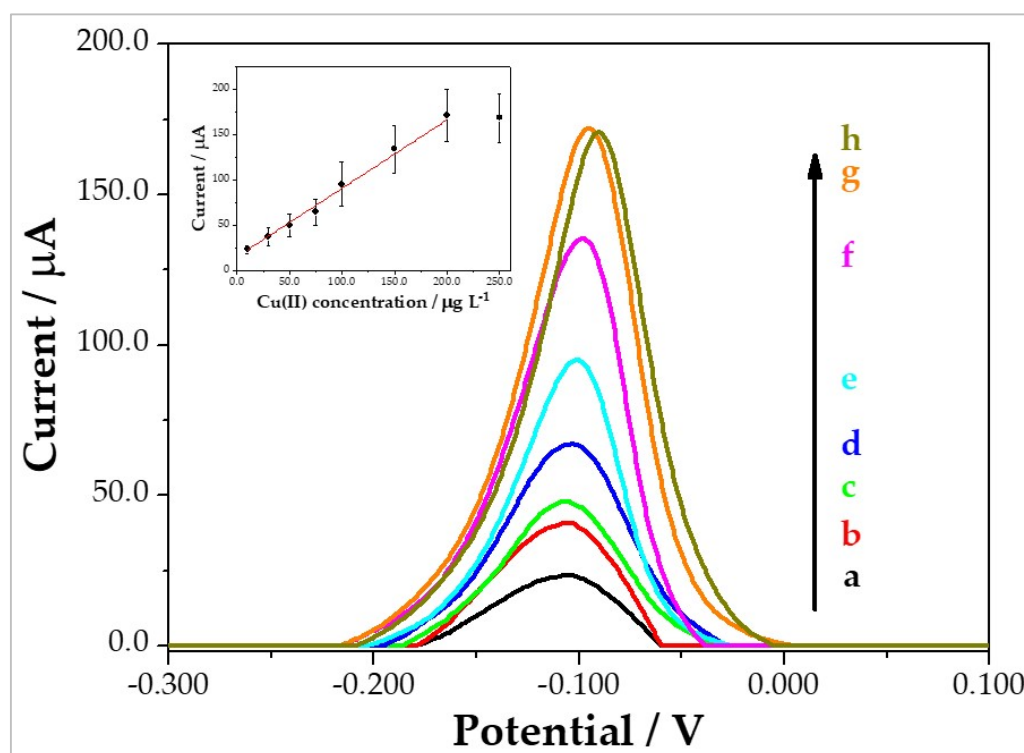


Figure 4. LSASV recordings at GCE/MWCNT-SB-dBA for increasing concentrations of Cu(II) from 10 to 250 $\mu\text{g L}^{-1}$. The inset shows the corresponding calibration plot. Experimental conditions as in Figure 1.

The selectivity of the sensor was evaluated by mixing Cu(II) with different cations at concentrations in high excess compared to the maximum levels allowed in drinking water [39,40]. Figure 5A displays linear scan voltammograms obtained in acetate buffer solution at the GCE/MWCNT-SB-dBA of the previous accumulation under the optimum conditions of 50 $\mu\text{g L}^{-1}$ Cu(II) in the presence of 5.0 $\mu\text{g L}^{-1}$ of Pb(II), Fe(II), As(III), Cr(III), Cd(II), or Hg(II). Figure 5B shows a bar plot for the oxidation peak currents obtained from the voltammograms presented in Figure 5A for Cu(II) alone and Cu(II) with 5.0 $\mu\text{g L}^{-1}$ of these cations. The percentage values of the currents obtained for Cu(II) in the presence of the different cations compared to those obtained for Cu(II) alone were 110.2, 95.9, 91.8, 92.0, 110.0, and 96.0 for Cu(II) with Pb(II), Fe(II), As(III), Cr(III), Cd(II), or Hg(II), respectively, indicating that the proposed electrochemical sensor is also very selective.

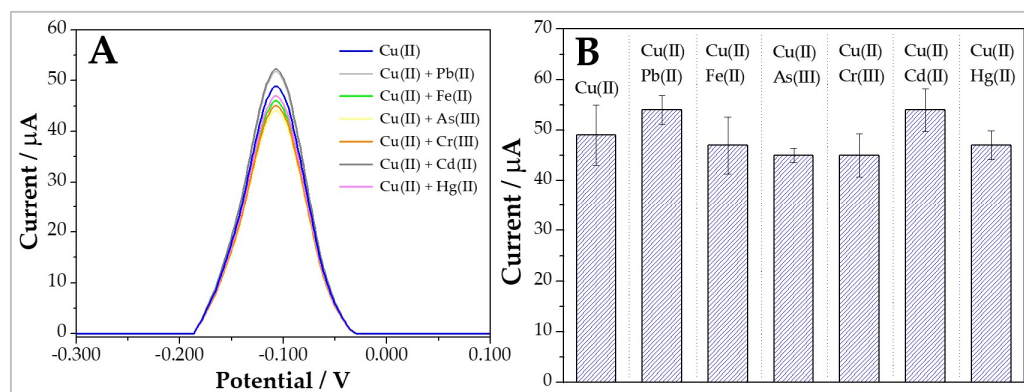


Figure 5. (A) LSASV response for $50 \mu\text{g L}^{-1}$ Cu(II) alone and in the presence of different cations ($5 \mu\text{g L}^{-1}$) and (B) the corresponding bar plot for the peak currents of the LSASVs shown in Figure 5A. Experimental conditions as in Figure 1.

To evaluate the practical usefulness of the sensor, we quantified Cu(II) in enriched samples of tap water, groundwater, and river water. Table 1 displays the recovery percentages obtained for samples enriched with 10 , 50 , and $100 \mu\text{g L}^{-1}$ Cu(II) (in triplicate). In tap water, the recovery percentages range between 96 and 104%; in groundwater, between 98 and 102%; in river water, these recovery values are between 97 and 107%. Therefore, GCE/MWCNT-SB-dBA could be successfully used for Cu(II) quantification in water samples in a simple, fast, sensitive, and selective way, opening the doors to future determinations of Cu(II) in different samples of environmental relevance.

Table 1. Recovery assay for Cu(II) from spiked tap water, groundwater, and river water samples using GCE/MWCNT-SB-dBA.

Real Sample	Spiked Cu(II)		
	$10 \mu\text{g L}^{-1}$	$50 \mu\text{g L}^{-1}$	$100 \mu\text{g L}^{-1}$
Tap water	$(96 \pm 3)\%$	$(104 \pm 4)\%$	$(98 \pm 2)\%$
Groundwater	$(102 \pm 2)\%$	$(98 \pm 3)\%$	$(99 \pm 1)\%$
River water	$(104 \pm 2)\%$	$(107 \pm 5)\%$	$(97 \pm 2)\%$

Table 2 summarizes the analytical parameters of the most relevant electrochemical Cu(II) sensors reported in recent years. The GCE/MWCNT-SB-dBA presents a better detection limit than most of the sensors included in the table [23,25,27,28,30,32,33,35–38]. The sensing platforms based on CCE and DA [22], GCE modified with Fe_3O_4 @PDA and DMSA [24], AuE modified with BMTCP or CPE containing BMTCP and AuNPs [26], GCE modified with a composite of ZnO and amino-functionalized Zr-based MOF [29], screen-printed platinum electrode (SPPtE) containing an electrosynthesized ion-imprinted polymer of PPD [31], and GCE modified with CMC and Nafion [34] presented lower detection limits than the electrochemical sensor proposed here. With the exception of [34], the preparation of other sensors requires long times and/or involves the synthesis of several compounds. For instance, the preparation of the ceramic electrode requires a long time [22]; the sensor reported in [24] involves several steps (synthesis of magnetite, further functionalization with DA and DMSA, and DA polymerization); the sensors proposed in [26] require, in one case, working with AuEs that need tedious pretreatments to ensure an efficient self-assembly of BMTCP, which takes 24 h, while in the other, involves the modification of a CPE with AuNPs previously synthesized and further functionalized with the chelating dithiol; the sensor based on a GCE modified with an amino-functionalized Zr-based MOF involves the synthesis of the MOF

and ZnO [29]; while in the case of [31], it is necessary to use expensive SPPtEs as a platform to grow the ion-imprinted polymer. Therefore, our sensor represents a very competitive alternative for the electrochemical sensing of Cu(II), through the efficient preconcentration on GCE/MWCNT-SB-dBA at ocp by exploiting the advantages of the $\text{Cu(II)} \cdots \text{N}_2\text{O}_2$ interaction that takes place in the SB-dBA support of MWCNTs.

Table 2. Comparison of the analytical performance of GCE/MWCNT-SB-dBA with other previously reported electrochemical sensors for Cu(II).

Platform	Technique	Linear Range	Detection Limit	Real Sample	Ref.
CCE/DA	DPASV	0.1–250 $\mu\text{g L}^{-1}$	0.03 $\mu\text{g L}^{-1}$	well water, tap water	[22]
CPE/MBT	SWASV	0.5–1.5 mg L^{-1} (500–1500 $\mu\text{g L}^{-1}$)	0.71 mg L^{-1} (710 $\mu\text{g L}^{-1}$)	tap water, drinking water	[23]
MGCE/ Fe_3O_4 @PDA-DMSA	DPV	0.5–50 $\mu\text{g L}^{-1}$	0.2 $\mu\text{g L}^{-1}$	lake water	[24]
GCE/MWCNT-BCS	DPASV	5.0×10^{-7} – 6.0×10^{-6} M (32–381 $\mu\text{g L}^{-1}$)	0.15 μM (9.5 $\mu\text{g L}^{-1}$)	tap water	[25]
AuE/BMTCPT	EIS	1.0×10^{-12} – 1.0×10^{-5} M (6.35×10^{-5} –635 $\mu\text{g L}^{-1}$)	9.7×10^{-13} M (6.2×10^{-5} $\mu\text{g L}^{-1}$)	groundwater	[26]
CPE-BMTCPT-AuNPs	POT	1.0×10^{-9} – 1.0×10^{-4} M (6.35×10^{-2} –6350 $\mu\text{g L}^{-1}$)	8.91×10^{-10} M (0.057 $\mu\text{g L}^{-1}$)		
GCE/MBs/eATA	SWV	1×10^{-6} – 1×10^{-4} M (63.5–6350 $\mu\text{g L}^{-1}$)	1.7×10^{-7} M (10.8 $\mu\text{g L}^{-1}$)	marsh water, sea water	[27]
GCE/Bi-MOF	DPV	1×10^{-5} – 1×10^{-1} M (635–6.35 $\times 10^6$ $\mu\text{g L}^{-1}$)	1×10^{-5} M (635 $\mu\text{g L}^{-1}$)	tap water	[28]
GCE/UiO-66-NH ₂ -ZnO	DPASV	0.2–0.9 μM (13–57 $\mu\text{g L}^{-1}$)	0.01435 μM (0.91 $\mu\text{g L}^{-1}$)	tap water	[29]
GCE/Zn/Ni-ZIF-8-XC72-Nf	DPV	0.397–19.9 ppm (397–19,900 $\mu\text{g L}^{-1}$)	0.0096 ppm (9.6 $\mu\text{g L}^{-1}$)	lake water, honey	[30]
SPPtE/eIIP based on PPD	DPV	0.95–244 nM (0.06–15.5 $\mu\text{g L}^{-1}$)	2.7 nM (0.17 $\mu\text{g L}^{-1}$)	drinking water	[31]
CPE-IIP based on MAH/EGDMA	DPASV	1.6–4.8 μM (102–305 $\mu\text{g L}^{-1}$)	1.4×10^{-7} M (8.9 $\mu\text{g L}^{-1}$)	mineral water, sea water	[32]
GCE/N-rGO/IIP based on Cys-CTS	DPASV	0.25–140 μM (16–8890 $\mu\text{g L}^{-1}$)	0.1 μM (6.3 $\mu\text{g L}^{-1}$)	tap water, bottled water, river water	[33]
GCE/CMC-Nf	SWV	1.0–50.0 nM (0.064–3.2 $\mu\text{g L}^{-1}$)	0.6 nM (0.038 $\mu\text{g L}^{-1}$)	tap water, lake water	[34]
CPE-aBC	DPASV	1.0–15.0 μM (63.5–952.5 $\mu\text{g L}^{-1}$)	0.36 μM (22.9 $\mu\text{g L}^{-1}$)	tap water	[35]
GCE/ZnSe-CdSe@SiO ₂ -Nf	AMP	100–900 $\mu\text{g L}^{-1}$	50 $\mu\text{g L}^{-1}$	---	[36]
CPE-MWCNT/NH ₂ -meso-Fe ₃ O ₄	DPV	1.0–70.0 μM (63.5–4445 $\mu\text{g L}^{-1}$)	0.6 μM (38.1 $\mu\text{g L}^{-1}$)	---	[37]
ISE based on CuS-PVC membrane	POT	1×10^{-6} – 1×10^{-1} M (63.5–6.35 $\times 10^6$ $\mu\text{g L}^{-1}$)	64 $\mu\text{g L}^{-1}$	---	[38]
GCE/MWCNT-SB-dBA	LSASV	10–200 $\mu\text{g L}^{-1}$	3.3 $\mu\text{g L}^{-1}$	tap water, groundwater, river water	This work

Abbreviations: CCE: carbon ceramic electrode; DA: dopamine; DPASV: differential pulse anodic stripping voltammetry; CPE: carbon paste electrode; MBT: 2-mercaptobenzothiazole; SWASV: square wave anodic stripping voltammetry; MGCE: magnetic glassy carbon electrode; Fe_3O_4 @PDA: magnetic polydopamine; DMSA: dimercaptosuccinic acid; DPV: differential pulse voltammetry; GCE: glassy carbon electrode; MWCNT: multiwall carbon nanotubes; BCS: bathocuproinedisulfonic acid; AuE: gold electrode; BMTCPT: bis(3-((5-mercapto-1,3,4-thiadiazol-2-yl)carbonyl)phenyl)terephthalate; EIS: electrochemical impedance spectroscopy; CPE: carbon paste electrode; AuNPs: gold nanoparticles; POT: potentiometry; GCE: glassy carbon electrode; MBs: magnetic beads; eATA: ammonium salt of aurintricarboxylic acid electrodeposited; SWV: square wave voltammetry; MOF: metal-organic framework; Bi-MOF: bismuth-containing MOF; UiO-66-NH₂: amino-functionalized zirconium-based MOF; ZIF-8: zinc-based zeolite imidazole framework; Zn/Ni-ZIF-8: nickel-substituted ZIF-8; XC72: VULCAN® XC72 carbon black; Nf: Nafion; SPPtE: screen-printed platinum electrode; IIP: ion-imprinted polymer; eIIP: IIP electrosynthesized; PPD: p-phenylenediamine; MAH: methacrylamido-L-histidine; EGDMA: ethylene glycol dimethacrylate; N-rGO: nitrogen-doped reduced graphene oxide; Cys-CTS: L-cysteine-grafted chitosan; CMC: sodium carboxymethyl cellulose; aBC: activated biochar; AMP: amperometry; NH₂-meso-Fe₃O₄: amine-functionalized mesoporous Fe₃O₄ nanoparticles; ISE: ion-selective electrode; PVC: polyvinyl chloride; LSASV: linear sweep anodic stripping voltammetry.

4. Conclusions

We reported a sensitive and selective electrochemical sensor for Cu(II) based on the advantageous combination of the catalytic properties of MWCNTs with the unique properties of the Schiff base (SB-dBA) rationally designed to efficiently exfoliate the carbon nanostructures and to work as a novel chelating agent for the preconcentration of Cu(II) through the complex formation at ocp. The huge increase in the electroactive area (due to the presence of the MWCNTs), the preconcentration of Cu(II) at the electrode surface (due to the presence of the N₂O₂ residues from the SB-dBA that supports the MWCNTs), and the improvement of the charge transfer (due to the presence of MWCNTs and the proximity of Cu(II)·SB-dBA complex to them) ensure the sensitive detection of Cu(II) (μg L⁻¹ levels) in a very simple and fast way. This new approach provides a rationally designed sensing platform for Cu(II) quantification at very competitive levels, offering interesting possibilities for environmental monitoring applications without the need for sample pretreatment, complicated protocols, and expensive instrumentation.

Author Contributions: Conceptualization, P.H.-I., P.D. and G.R.; methodology, A.T., M.L.M. and G.S.; validation, P.H.-I., P.D. and G.R.; formal analysis, A.T., M.L.M. and G.S.; investigation, A.T. and M.L.M.; resources, G.S., P.H.-I. and G.R.; writing—original draft preparation, P.D. and G.R.; writing—review and editing, D.V.-Y., P.H.-I., P.D. and G.R.; visualization, A.T. and M.L.M.; supervision, P.H.-I., P.D. and G.R.; funding acquisition, P.H.-I., P.D. and G.R. All authors have read and agreed to the published version of the manuscript.

Funding: This research was funded by ANPCyT-FONCyT (PICT 2019-01114), CONICET (PIP 2022-11220210100957CO), SCTyP-UTN (PID MSEC00010216TC), and SECyT-UNC (PIDTA 2023) from Argentina, and Financiamiento Basal Program CEDENNA, FONDECYT Iniciación 11190540, and ANID-Fondecyt Grant N° 1250720 from Chile.

Institutional Review Board Statement: Not applicable.

Informed Consent Statement: Not applicable.

Data Availability Statement: Data are contained within the article.

Acknowledgments: The authors thank the financial and institutional support of ANPCyT, CONICET, SCTyP-UTN, SECyT-UNC from Argentina, and ANID-Fondecyt from Chile. A.T. and M.L.M. acknowledge their fellowships to CONICET. P.D. and G.R. are members of the Research Career of CONICET.

Conflicts of Interest: The authors declare no conflicts of interest.

References

1. Srivastava, A.; Azad, U.P. Nanobioengineered surface comprising carbon based materials for advanced biosensing and biomedical application. *Int. J. Biol. Macromol.* **2023**, *253*, 126802. [[CrossRef](#)] [[PubMed](#)]
2. Maduraiveeran, G.; Jin, W. Carbon nanomaterials: Synthesis, properties and applications in electrochemical sensors and energy conversion systems. *Mater. Sci. Eng. B* **2021**, *272*, 115341. [[CrossRef](#)]
3. Speranza, G. Carbon nanomaterials: Synthesis, functionalization and sensing applications. *Nanomaterials* **2021**, *11*, 967. [[CrossRef](#)] [[PubMed](#)]
4. Flores-Lasluisa, J.X.; Navlani-García, M.; Berenguer-Murcia, A.; Morallón, E.; Cazorla-Amorós, D. 10 Years of frontiers in carbon-based materials: Carbon, the “newest and oldest” material. The story so far. *Front. Mater.* **2024**, *11*, 1381363. [[CrossRef](#)]
5. Ferrier, D.C.; Honeychurch, K.C. Carbon nanotube (CNT)-based biosensors. *Biosensors* **2021**, *11*, 486. [[CrossRef](#)] [[PubMed](#)]
6. Gutierrez, F.; Rubianes, M.D.; Rivas, G.A. New bioanalytical platform based on the use of avidin for the successful exfoliation of multi-walled carbon nanotubes and the robust anchoring of biomolecules. Application for hydrogen peroxide biosensing. *Anal. Chim. Acta* **2019**, *1065*, 12–20. [[CrossRef](#)]
7. Eguílaz, M.; Gutierrez, A.; Rivas, A. Non-covalent functionalization of multi-walled carbon nanotubes with cytochrome c: Enhanced direct electron transfer and analytical applications. *Sens. Actuators B Chem.* **2016**, *216*, 629–637. [[CrossRef](#)]

8. Dalmasso, P.R.; Pedano, M.L.; Rivas, G.A. Dispersion of multi-wall carbon nanotubes in polyhistidine: Characterization and analytical applications. *Anal. Chim. Acta* **2012**, *710*, 58–64. [[CrossRef](#)]
9. López Mujica, M.; Tamborelli, A.; Espinosa, C.; Vaschetti, V.; Bollo, S.; Dalmasso, P.; Rivas, G. Two birds with one stone: Integrating exfoliation and immunoaffinity properties in multi-walled carbon nanotubes by non-covalent functionalization with human immunoglobulin G. *Microchim. Acta* **2023**, *190*, 73. [[CrossRef](#)] [[PubMed](#)]
10. Ortiz, E.; Gallay, P.; Galicia, L.; Eguílaz, M.; Rivas, G. Nanoarchitectures based on multi-walled carbon nanotubes non-covalently functionalized with Concanavalin A: A new building-block with supramolecular recognition properties for the development of electrochemical biosensors. *Sens. Actuators B Chem.* **2019**, *292*, 254–262. [[CrossRef](#)]
11. Zhou, N.; Cai, M.; Zheng, S.; Guo, H.; Yang, F. First organic fluorescent sensor for pesticide paclobutrazol based on tetraphenylimidazole Schiff base. *Sens. Actuators B Chem.* **2024**, *417*, 136051. [[CrossRef](#)]
12. Willery, M.; Julliard, P.-G.; Molton, F.; Thomas, F.; Fortage, J.; Costentin, C.; Collomb, M.-N. Mechanism of electrochemical proton reduction catalyzed by a cobalt tetraaza Schiff base macrocyclic complex: Ligand protonation and/or influence of the chloro ligand. *ACS Catal.* **2024**, *14*, 11352–11365. [[CrossRef](#)]
13. Gu, Z.-X.; Zhang, N.; Zhang, Y.; Liu, B.; Jiang, H.-H.; Xu, H.-M.; Wang, P.; Jiang, Q.; Xiong, R.-G.; Zhang, H.-Y. Molecular orbital breaking in photo-mediated organosilicon Schiff base ferroelectric crystals. *Nat. Commun.* **2024**, *15*, 4416. [[CrossRef](#)]
14. Belay, Y.; Muller, A.; Mokoena, F.S.; Adeyinka, A.S.; Motadi, L.R.; Oyebamiji, A.K. 1,2,3-Triazole and chiral Schiff base hybrids as potential anticancer agents: DFT, molecular docking and ADME studies. *Sci. Rep.* **2024**, *14*, 6951. [[CrossRef](#)] [[PubMed](#)]
15. Tamborelli, A.; López Mujica, M.; Sánchez-Velasco, O.A.; Hormazábal-Campos, C.; Pérez, E.G.; Gutierrez-Cutiño, M.; Venegas-Yazigi, D.; Dalmasso, P.; Rivas, G.; Hermosilla-Ibáñez, P. A New Strategy to build electrochemical enzymatic biosensors using a nanohybrid material based on carbon nanotubes and a rationally designed Schiff base containing boronic acid. *Talanta* **2024**, *270*, 125520. [[CrossRef](#)] [[PubMed](#)]
16. Tamborelli, A.; Vaschetti, V.; Viada, B.; López Mujica, M.; Bollo, S.; Venegas-Yazigi, D.; Hermosilla-Ibáñez, P.; Rivas, G.; Dalmasso, P. Multi-walled carbon nanotubes functionalized with a new Schiff base containing phenylboronic acid residues: Application to the development of a bienzymatic glucose biosensor using a response surface methodology approach. *Microchim. Acta* **2024**, *191*, 558. [[CrossRef](#)]
17. Groom, C.R.; Bruno, I.J.; Lightfoot, M.P.; Ward, S.C. The Cambridge Structural Database. *Acta Crystallogr. B Struct. Sci. Cryst. Eng. Mater.* **2016**, *72*, 171–179. [[CrossRef](#)] [[PubMed](#)]
18. Da Costa Ferreira, A.M.; Hureau, C.; Facchin, G. Bioinorganic chemistry of copper: From biochemistry to pharmacology. *Inorganics* **2024**, *12*, 97. [[CrossRef](#)]
19. Rehman, M.; Liu, L.; Wang, Q.; Saleem, M.H.; Bashir, S.; Ullah, S.; Peng, D. Copper environmental toxicology, recent advances, and future outlook: A review. *Environ. Sci. Pollut. Res.* **2019**, *26*, 18003–18016. [[CrossRef](#)]
20. Liu, Y.; Wang, H.; Cui, Y.; Chen, N. Removal of copper ions from wastewater: A review. *Int. J. Environ. Res. Public Health* **2023**, *20*, 3885. [[CrossRef](#)]
21. Brewer, G.J. Avoiding Alzheimer's disease: The important causative role of divalent copper ingestion. *Exp. Biol. Med.* **2019**, *244*, 114–119. [[CrossRef](#)]
22. Rohani, T.; Mohammadi, S.Z.; Zadeh, N.G. Sensitive detection of trace amounts of copper by a dopamine modified carbon ceramic electrode. *Polyhedron* **2019**, *168*, 88–93. [[CrossRef](#)]
23. Flores-Álvarez, J.M.; Cortés-Arriagada, D.; Reyes-Gómez, J.; Gómez-Sandoval, Z.; Rojas Montes, J.C.; Pineda-Urbina, K. 2-Mercaptobenzothiazole modified carbon paste electrode as a novel copper sensor: An electrochemical and computational study. *J. Electroanal. Chem.* **2021**, *888*, 115208. [[CrossRef](#)]
24. Wang, L.; Jiang, X.; Su, S.; Rao, J.; Ren, Z.; Lei, T.; Bai, H.; Wang, S. A thiol and magnetic polymer-based electrochemical sensor for on-site simultaneous detection of lead and copper in water. *Microchem. J.* **2021**, *168*, 106493. [[CrossRef](#)]
25. Saldaña, J.; Gallay, P.; Gutierrez, S.; Eguílaz, M.; Rivas, G. Multi-walled carbon nanotubes functionalized with bathocuproinedisulfonic acid: Analytical applications for the quantification of Cu(II). *Anal. Bioanal. Chem.* **2020**, *412*, 5089–5096. [[CrossRef](#)] [[PubMed](#)]
26. Kaur, I.; Sharma, M.; Kaur, S.; Kaur, A. Ultra-sensitive electrochemical sensors based on self-assembled chelating dithiol on gold electrode for trace level detection of copper(II) ions. *Sens. Actuators B Chem.* **2020**, *312*, 127935. [[CrossRef](#)]
27. Ben Ali Hassine, C.; Bourourou, M.; Barhoumi, H.; Jaffrezic, N. Copper(II) electrochemical sensor based on Aluminon as chelating ionophore. *IEEE Sens. J.* **2019**, *19*, 8605–8611. [[CrossRef](#)]
28. Theerthagiri, S.; Rajkannu, P.; Kumar, P.S.; Peethambaram, P.; Ayyavu, C.; Rasu, R.; Kannaiyan, D. Electrochemical sensing of copper (II) ion in water using bi-metal oxide framework modified glassy carbon electrode. *Food Chem. Toxicol.* **2022**, *167*, 113313. [[CrossRef](#)]
29. Li, Z.; Li, Q.; Jiang, R.; Qin, Y.; Luo, Y.; Li, J.; Kong, W.; Yang, Z.; Huang, C.; Qu, X.; et al. An electrochemical sensor based on a MOF/ZnO composite for the highly sensitive detection of Cu(II) in river water samples. *RSC Adv.* **2022**, *12*, 5062. [[CrossRef](#)]

30. Li, D.; Qiu, X.; Guo, H.; Duan, D.; Zhang, W.; Wang, J.; Ma, J.; Ding, Y.; Zhang, Z. A simple strategy for the detection of Pb(II) and Cu(II) by an electrochemical sensor based on Zn/Ni-ZIF-8/XC-72/Nafion hybrid materials. *Environ. Res.* **2021**, *202*, 111605. [[CrossRef](#)]
31. Di Masi, S.; Pennetta, A.; Guerreiro, A.; Canfarotta, F.; De Benedetto, G.E.; Malitesta, C. Sensor based on electrosynthesised imprinted polymeric film for rapid and trace detection of copper(II) ions. *Sens. Actuators B Chem.* **2020**, *307*, 127648. [[CrossRef](#)]
32. Sala, A.; Ibrahim, F.; Lenoble, V.; D'Onofrio, S.; Margaillan, A.; Mullot, J.-U.; Brisset, H.; Branger, C. Design of an histidine-based imprinted polymer as a selective receptor of copper(II) for its detection in seawater. *React. Funct. Polym.* **2024**, *195*, 105809. [[CrossRef](#)]
33. Gong, S.; Liu, X.; Liao, H.; Lin, X.; Huang, Q.; Hasan, M.; Shu, X.; Zhou, X.; Gunasekaran, S. Tailoring of L-cysteine conjugated chitosan carbon electrode for selective and sensitive monitor of copper in the water. *Mater. Today Commun.* **2023**, *35*, 106092. [[CrossRef](#)]
34. Wang, J.; Liu, D.; Liu, Y.; Wang, F.; Huang, S.; Luo, X.; Liu, D.; Chen, D.; Wei, J.; Ning, J. Highly hydrophilic polymer composite modified electrode for trace copper detection based on synergetic electrostatic attractions and chelating interactions. *Electroanalysis* **2020**, *32*, 2273–2281. [[CrossRef](#)]
35. Pianaro Valenga, M.G.; Gevaerd, A.; Marcolino-Junior, L.H.; Bergamini, M.F. Biochar from sugarcane bagasse: Synthesis, characterization, and application in an electrochemical sensor for copper (II) determination. *Biomass Bioenergy* **2024**, *184*, 107206.
36. Bakhsh, E.M.; Khan, S.B.; Marwani, H.M.; Danish, E.Y.; Asiri, A.M. Efficient electrochemical detection and extraction of copper ions using ZnSe–CdSe/SiO₂ core–shell nanomaterial. *J. Ind. Eng. Chem.* **2019**, *73*, 118–127. [[CrossRef](#)]
37. Noroozi, S.; Hashemnia, S.; Mokhtari, Z. Facile synthesis of cube-shaped Fe₃O₄ mesoporous nanoparticles and their application for electrochemical determination of Cu(II) in aqueous solutions through the mediating effect of indigo carmine. *Mater. Sci. Eng. B* **2022**, *286*, 116057. [[CrossRef](#)]
38. Gupta, D.K.; Neupane, S.; Yadav, H.C.; Subedi, V.; Singh, S.; Yadav, R.J.; Das, A.K.; Yadav, B.; Nakarmi, K.B.; Karki, N.; et al. Trace level monitoring of Cu(II) ion using CuS particles based membrane electrochemical sensor. *Heliyon* **2021**, *7*, e07167. [[CrossRef](#)] [[PubMed](#)]
39. National Primary Drinking Water Regulations. Available online: <https://www.epa.gov/ground-water-and-drinking-water/national-primary-drinking-water-regulations#Inorganics> (accessed on 30 December 2024).
40. Secondary Drinking Water Standards: Guidance for Nuisance Chemicals. Available online: <https://www.epa.gov/sdwa/secondary-drinking-water-standards-guidance-nuisance-chemicals> (accessed on 30 December 2024).

Disclaimer/Publisher's Note: The statements, opinions and data contained in all publications are solely those of the individual author(s) and contributor(s) and not of MDPI and/or the editor(s). MDPI and/or the editor(s) disclaim responsibility for any injury to people or property resulting from any ideas, methods, instructions or products referred to in the content.